# Diversity and Wiring Variability of Olfactory Local Interneurons in the *Drosophila* Antennal Lobe

Ya-Hui Chou, Maria L. Spletter, Emre Yaksi, Jonathan C. S. Leong, Rachel I. Wilson, Liqun Luo

Nature Neuroscience: doi:10.1038/nn.2489

# Supplementary Table 1

| | HB 4-93 | NP6277 | H24 | GH298 | NP3056 | HB 8-145 | LCCH3-Gal4 | Nan-Gal4 | Krasavietz-Gal4 | OK107 | | Average No of cells/AL | | | No of ALs |
|---|---|---|---|---|---|---|---|---|---|---|---|---|---|---|---|
| | Line1 | Line2 | Line3 | Line4 | Line5 | Line6 | Line7 | Line8 | Line9 | Line10 | | GABA+ | GABA–Cha+ | GABA–Cha- | |
| Line1 | 35±3 | | | | | | | | | | Line1 | | | | |
| Line2 | | (519±30) | 96 ± 8 | | | | | | | | Line2 | | | | |
| Line3 | 49±2 | | 30±3 | | | | | | | | Line3 | 29±2 | 1±1 | 0.1±0.3 | 10 |
| Line4 | 45±4 | | 48±2 | 28±2 | | | | | | | Line4 | 24±2 | 1±1 | 0.1±0.3 | 10 |
| Line5 | 70±4 | | 76±11 | 73±7 | 56±4 | | | | | | Line5 | 42±10 | 2±3 | 14±9 | 10 |
| Line6 | | | 30±1 | 33±3 | 55±4 | 7±1 | | | | | Line6 | 7±1 | 0 | 0.4±0.5 | 10 |
| Line7 | | | 51±3 | 54±6 | 56±3 | 27±6 | 30±8 | | | | Line7 | 20±6 | 0.3±0.9 | 5±5 | 12 |
| Line8 | | | 34±1 | 36±3 | 56±10 | 12±1 | 30±4 | 5±1 | | | Line8 | 3±3 | 0.2±0.5 | 1±1 | 24 |
| Line9 | | | | 37±3 | 56±5 | 20±3 | 43±9 | 20±4 | 16±4 | | Line9 | 12±3 | 2±1 | 5±2 | 10 |
| Line10 | | | | | 162±11 | | | | | 103±10 | Line10 | 54±13 | 1±1 | 33 ±6 | 6 |

**Supplementary Table 1. Estimated number of LNs labeled by individual Gal4 lines and their neurotransmitter profiles.**
Estimate of the number (±SD) of LNs labeled by individual Gal4 lines (yellow blocks) and their combinations, based on scoring from *n*=7-16 antennal lobes. The cell number labeled by the combination of Lines 3, 4 and 5 is above the yellow blocks. Numbers (in parentheses) for Line2 include all labeled neurons near the antennal lobe; the rest are estimates of LNs (see **Supplementary Fig. 1**). The breakdown of the numbers by GABA and Cha expression is given on the right (±SD). AL, antennal lobe.
Note: Fewer cells are labeled by GH298 in our study than two previous reports[1,2]. This is because we excluded from our cell counts GABA-negative Cha-positive PNs according to our MARCM analysis. Our finding that most krasavietz LNs are GABA+ disagrees with a previous study[2], which reported that only 39% of the LNs labeled by this Gal4 line are GABA+. Similar counts of GABA+ cells in this line were obtained independently in the Luo and Wilson labs.

# Supplementary Tables 2 and 3
(See separate Excel sheets)

**Supplementary Table 2. Raw data for ipsilateral glomerular innervation patterns.**
We present our raw scoring data of ipsilateral innervation pattern as a 54 X 1532 matrix, with additional columns to the left of the 54 glomeruli listing available data for GABA staining, birth timing, cell type, and Gal4 lines used. Each cell is identified by a unique number in the first column. Cells are sorted first by Gal4, then by birth time and finally by cell type. 1 represents "innervated" and 0 represents "not innervated."

**Supplementary Table 3. Raw data for contralateral glomerular innervation patterns of bilateral projection LNs.**
We present our raw scoring data of contralateral innervation patterns of bilateral projection LNs as a 54 X 43 matrix. Columns to the left of the glomeruli list data as in **Supplementary Table 2**. Corresponding ipsilateral projections of these cells can be identified in **Supplementary Table 2** by the same ID number in the first row. Cells are sorted first by Gal4, then by birth time and finally by cell type. 1 represents "innervated" and 0 represents "not innervated."

# Supplementary Table 4

| | | | | | | |
|---|---|---|---|---|---|---|
| **fig. 2a** (left to right) | Line5 (*NP3056*) | Line4 (*GH298*) | Line6 (*HB8-145*) | Line5 (*NP3056*) | Line5 (*NP3056*) | Line5 (*NP3056*) |
| **fig. 2b** (left to right) | Line5 (*NP3056*) | Line6 (*HB8-145*) | Line1 (*HB4-93*) | Line1 (*HB4-93*) | Line3 (*H24*) | Line5 (*NP3056*) |
| **fig. 2c** (left to right) | Line3 (*H24*) | Line5 (*NP3056*) | Line5 (*NP3056*) | Line5 (*NP3056*) | Line9 (*krasavietz-Gal4*) | Line1 (*HB4-93*) |
| **fig. 2d** (left to right) | Line1 (*HB4-93*) | Line1 (*HB4-93*) | Line1 (*HB4-93*) | Line1 (*HB4-93*) | Line5 (*NP3056*) | Line5 (*NP3056*) |
| **fig. 2e** (left to right) | Line3 (*H24*) | Line5 (*NP3056*) | Line5 (*NP3056*) | Line5 (*NP3056*) | Line10 (*OK107*) | Line10 (*OK107*) |
| **fig. 2f** (left to right) | Line10 (*OK107*) | Line10 (*OK107*) | Line3 (*H24*) | Line10 (*OK107*) | Line5 (*NP3056*) | Line5 (*NP3056*) |
| **fig. 3c** (left to right) | Line6 (*HB8-145*) | | Line6 (*HB8-145*) | | Line3 (*H24*) | |
| **fig. 3d** (left to right) | Line1 (*HB4-93*) | | Line1 (*HB4-93*) | | Line1 (*HB4-93*) | |
| **fig. 3e** (left to right) | Line1 (*HB4-93*) | | Line1 (*HB4-93*) | | Line1 (*HB4-93*) | |
| **fig. 7c-h** | *hsFLP/+; FRT40A/tub-Gal80 FRT40A; UAS>CD2 y$^{+}$>mCD8GFP/NP3056* | | | | | |
| **fig. 8a** | *UAS-mCD8GFP hsFLP/+; smo$^{3}$ FRT40A/tub-Gal80 FRT40.* | | | | | |
| **fig. 8b** | *UAS-mCD8GFP hsFLP/+; smo$^{3}$ FRT40A/tub-Gal80 FRT40A; NP3056/* | | | | | |
| **fig. 8c** | *UAS-mCD8GFP hsFLP/+; smo$^{3}$ FRT40A/tub-Gal80 FRT40A GH146-Gal4* | | | | | |
| **fig. 8e** | *UAS-mCD8GFP UAS-sytHA hsFLP122/+; FRT40A/tub-Gal80 FRT40A; HB8-145/+* | | | | | |
| **fig. S5** Pan-glomerular (left to right) | Line1 (*HB4-93*) | | Line1 (*HB4-93*) | | Line1 (*HB4-93*) | |
| **fig. S5** Pheromonal avoiding (left to right) | Line6 (*HB8-145*) | | Line3 (*H24*) | | Line6 (*HB8-145*) | |
| **fig. S5** DM avoiding (left to right) | Line5 (*NP3056*) | | Line5 (*NP3056*) | | Line5 (*NP3056*) | |
| **fig. S5** DA avoiding (left to right) | Line1 (*HB4-93*) | | Line3 (*H24*) | | Line3 (*H24*) | |
| **fig. S5** Patchy (left to right) | Line1 (*HB4-93*) | | Line1 (*HB4-93*) | | Line1 (*HB4-93*) | |
| **fig. S5** Dumbbell (left to right) | Line1 (*HB4-93*) | | Line1 (*HB4-93*) | | Line1 (*HB4-93*) | |
| **fig. S5** Lateral (left to right) | Line3 (*H24*) | | Line2 (*NP6277*) | | Line2 (*NP6277*) | |
| **fig. S5** Posterior (left to right) | Line3 (*H24*) | | Line3 (*H24*) | | Line3 (*H24*) | |
| **fig. S5** Few-glomerular (left to right) | Line1 (*HB4-93*) | | Line3 (*H24*) | | Line1 (*HB4-93*) | |
| **fig. S10** | Line 5 (*NP3056*) | | | | | |

**Supplementary Table 4. Gal4 line information and genotypes for all images shown in Fig. 2-3, 7-8 and Supplementary Fig. 5 and 10.**

Supplementary Figure 1

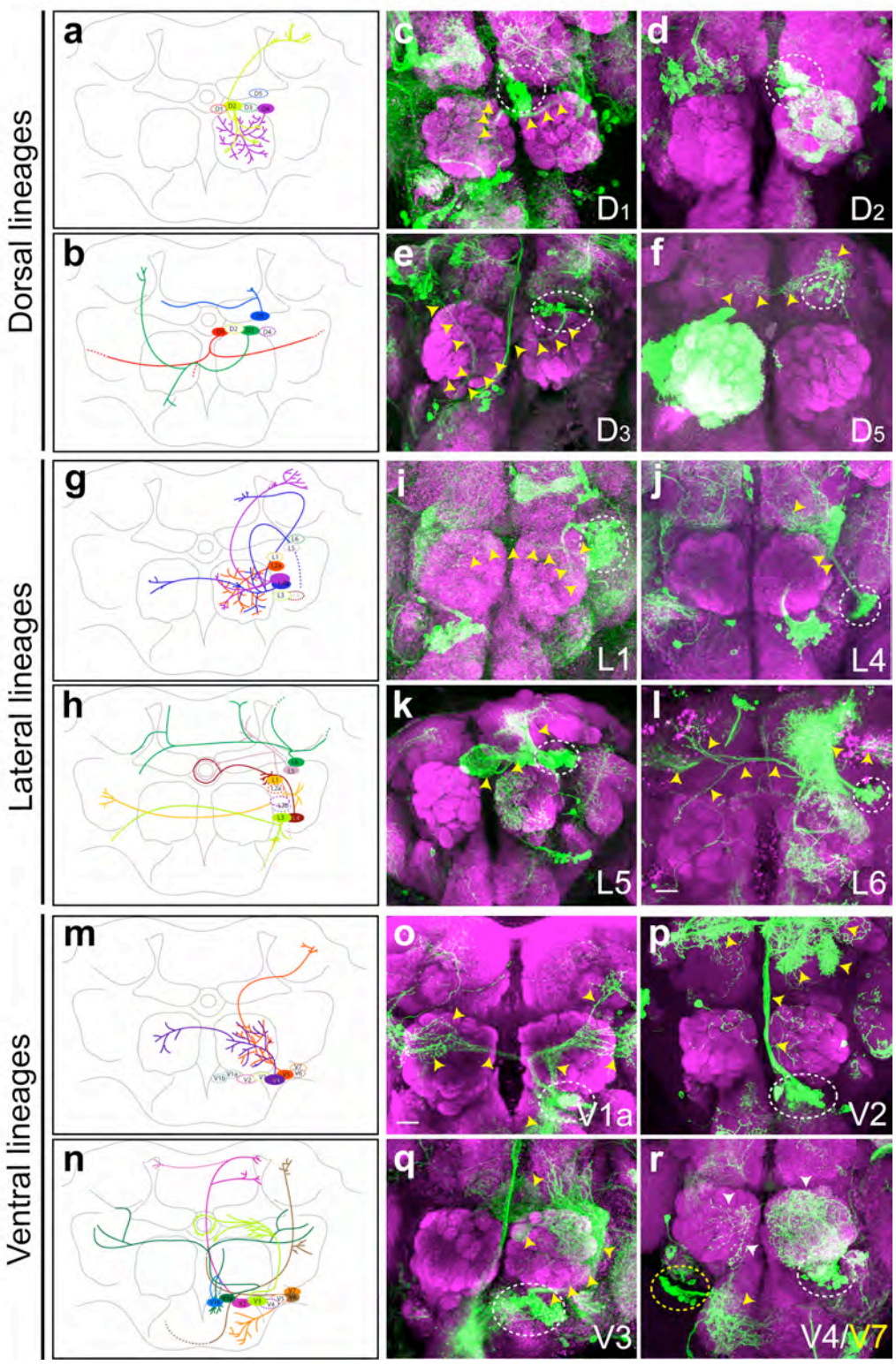


**Supplementary Figure 1. Neuroblast organization of neurons near the antennal lobe.** Some of the 10 LN Gal4 lines used in this study also label additional cell types as judged both from Gal4 expression patterns and MARCM clonal analysis. Line2 is broadly expressed in many cell types near the antennal lobe as well as ORNs. Additionally, Lines 1, 4, 6 and 8 are expressed in a subset of ORNs; Lines 1, 3 and 4 are expressed in a subset of PNs; Lines 3

and 9 are expressed in a subset of mushroom body neurons[3,4] and Line10 (OK107) is expressed in all mushroom body neurons[5]. The data summarized in this figure are grouped into dorsal (D), lateral (L) and ventral (V) clusters, based mostly on neuroblast clones labeled by Line2 (with some contribution by Line1), provide information about LNs as well as other neurons near the antennal lobe with regard to their approximate cell body locations and potential neuroblast lineages. Potential lineages are named alphanumerically based on their cell body position. Such information might be useful for future comprehensive mapping of neurons in the *Drosophila* brain.

(**a-b**) Schemes illustrating the projection patterns of dorsal neuroblasts with (**a**) or without (**b**) innervation in the antennal lobe. Lineage D1 neurons project bilaterally to the lateral regions of both brain hemispheres. D2 neurons are typical anterodorsal PNs. D3 neurons have 2 axon branches targeting to the SOG (suboesophageal ganglion) and a dorsoanterior neuropil. The majority of D4 neurons are LNs. D5 neurons have 2 axon braches projecting ispilaterally to the region near the peduncle of the mushroom body (MB), and bilaterally to both MB β lobes.

(**c-f**) Examples showing the projections of 4 dorsal neuroblast clones (lineage D1, D2, D3 and D5, respectively) labeled by Line2. Green, mCD8GFP; magenta, nc82. Dashed lines mark the cell bodies of each neuroblast clone. Arrowheads indicate a part of the axonal path of the neuroblasts.

(**g-h**) Schemes illustrating the projection patterns of lateral neuroblasts with (**g**) or without (**h**) innervation in the antennal lobe. L1 neurons have 3 axon branches targeting to a lateral neuropil bilaterally and an ipsilateral ventral neuropil. The majority of L2a neurons are LNs. L2b neurons include typical lateral PNs and atypical PNs, which innervate ipsilateral and contralateral antennal lobes and project axons to different higher brain centers. L2a and L2b may derive from the same neuroblast[6]. L3 neurons innervate the AMMC (antennal motor and mechanosensory center) bilaterally and an ipsilateral neuropil next to AMMC. L4 neurons project axons to the lateral accessory lobe and ellipsoid body. L5 neurons have axons targeting to the central complex, a ventroposterior neuropil and a neuropil next to the dorsal lobe of MB. L6 neurons bilaterally project to dorsolateral neuropils close to the dorsal and medial lobes of MBs.

(**i-l**) Examples showing the projections of 4 lateral neuroblast clones (lineage L1, L4, L5 and L6, respectively) labeled by Line2 (**i-k**) and Line1 (**l**). Green, mCD8GFP; magenta, nc82. Dashed lines mark the cell bodies of each neuroblast clone. Arrowheads indicate a part of the axonal path of the neuroblasts. Scale bar, 20 μm.

(**m-n**) Schemes illustrating the projection patterns of ventral neuroblasts with (**m**) or without (**n**) innervation in the antennal lobe. V1a neurons have axons bilaterally targeting to a lateral neuropil. V1b neurons project to a ventroposterior neuropil. It is unclear whether V1a and V1b neurons derive from the same neuroblast. V2 neurons have axons targeting to the head and the trunk of the MB dorsal lobes. Occasionally in bigger neuroblast clones, an additional branch projecting to the head of the contralateral MB dorsal lobe was observed. V3 neurons innervate the lateral accessory lobe, ellipsoid body and noduli. The majority of V4 neurons are LNs with bilateral innervation, but a few of them have only ispilateral innervation. V5 neurons include typical and atypical PNs. V6 neurons have 3 axon branches targeting to the SOG bilaterally, a medial region posterior to the antennal lobe, and a lateral and a dorsal neuropil. V7 neurons innervate the SOG.

(**o-r**) Examples showing the projections of 5 ventral neuroblast clones (lineage V1a, V2, V3, V4 and V7, respectively) labeled by Line1 (**o**) and Line2 (**p-r**). Green, mCD8GFP; magenta, nc82. Dashed lines mark the cell bodies of each neuroblast clone. Arrowheads indicate a part of the axonal path of the neuroblasts. Scale bar, 20 μm.

Representative confocal stacks can be found at http://flybrain.stanford.edu**.**

Supplementary Figure 2

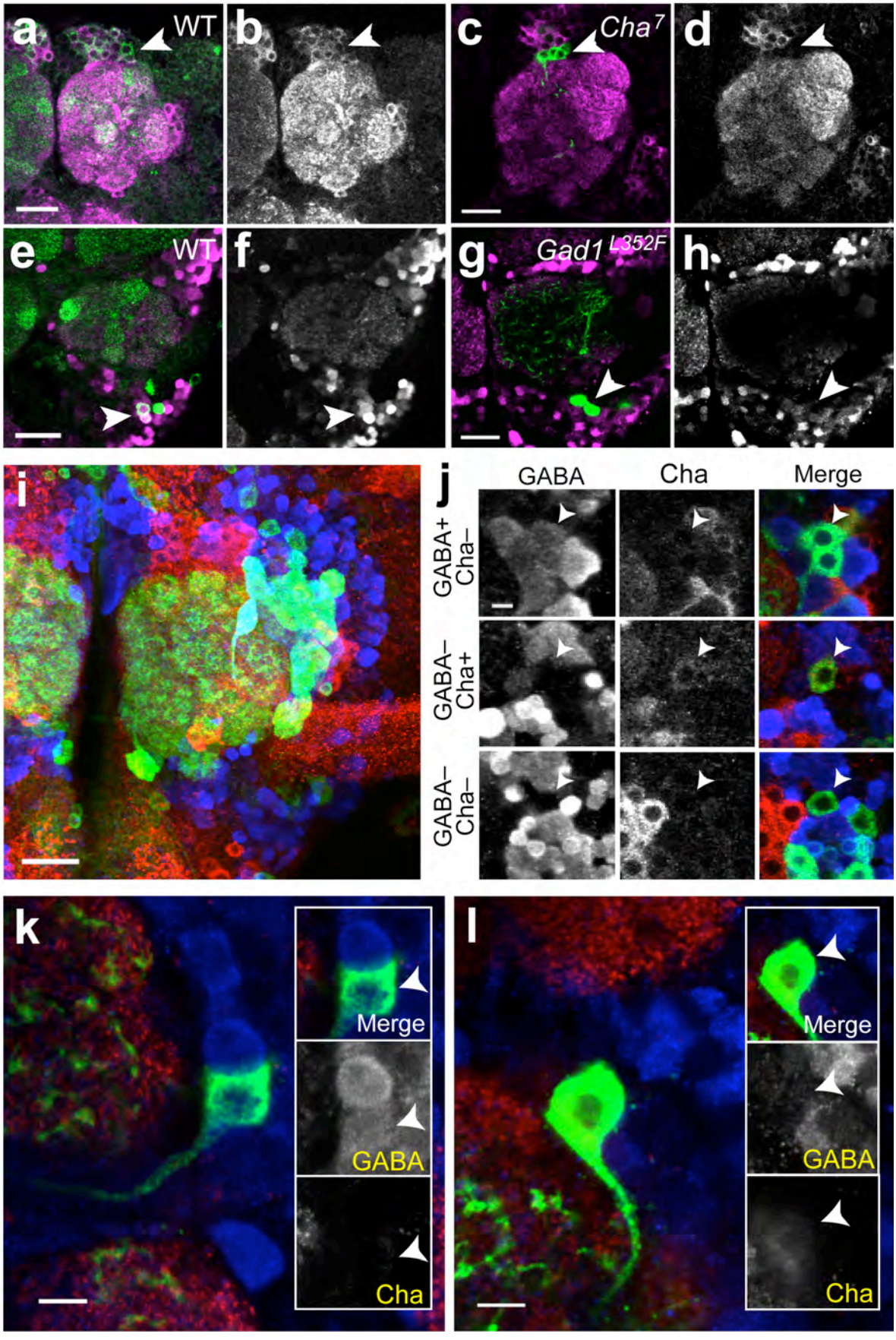

**Supplementary Figure 2. GABAergic and cholinergic LNs.**

(**a-d**) Genetic confirmation that anti-Cha antibody specifically recognizes Choline acetyltransferase. Anti-Cha antibody stains anterodorsal GH146-Gal4 positive PNs (arrowheads in **a**, **b**), but the staining is abolished in an anterodorsal neuroblast clone homozygous for *Cha*$^{7}$ (arrowheads in **c**, **d**)[7]. (**a**) and (**c**) are labeled in magenta with anti-Cha antibody and in green with UAS-mCD8GFP driven from GH146-Gal4 (**a**) or GH146-Gal4 based MARCM (**c**). (**b**) and (**d**) show only the anti-Cha channel from (**a**) and (**c**), respectively. Scale bars, 20 μm.

(**e-h**) Genetic confirmation that anti-GABA antibody specifically recognizes GABA. Anti-GABA antibody stains GH146-Gal4 positive ventral PNs (arrowheads in **e**, **f**)[8], but the staining is abolished in a ventral neuroblast clone homozygous for *Gad1*$^{L352F}$ (arrowheads in **g**, **h**)[9]. (**e**) and (**f**) are labeled in magenta with anti-GABA antibody and in green with UAS-mCD8GFP driven from GH146-Gal4 (**e**) or GH146-Gal4 based MARCM (**g**). (**f**) and (**h**) show only the anti-GABA channels for (**e**) and (**g**), respectively. Scale bars, 20 μm.

(**i-j**) Representative images of LNs stained with Cha and GABA. (**i**) Z projection of a Line5 Gal4 driven mCD8GFP brain shows GFP (green), Cha (red) and GABA (blue) staining. (**j**) Single confocal sections from Line5 labeled LNs showing examples of GABA-positive Cha-negative, GABA-negative Cha-positive and GABA-negative Cha-negative LNs as indicated by arrowheads. Scale bars, 20 μm (**i**) and 5 μm (**j**).

(**k-l**) Representative images of single LN cell clones stained with Cha and GABA. The projections of a GABA-positive (**k**) and a GABA-negative (**l**) cell show Line1 driven mCD8-GFP (green), GABA (blue) and Cha (red) staining. Both cells are Cha-negative. Insets show images of the cell bodies (arrowheads) with GFP (green in top panels), GABA (blue in top and alone in middle panels) and Cha (red in top and alone in bottom panels). Scale bars, 5 μm.

Supplementary Figure 3

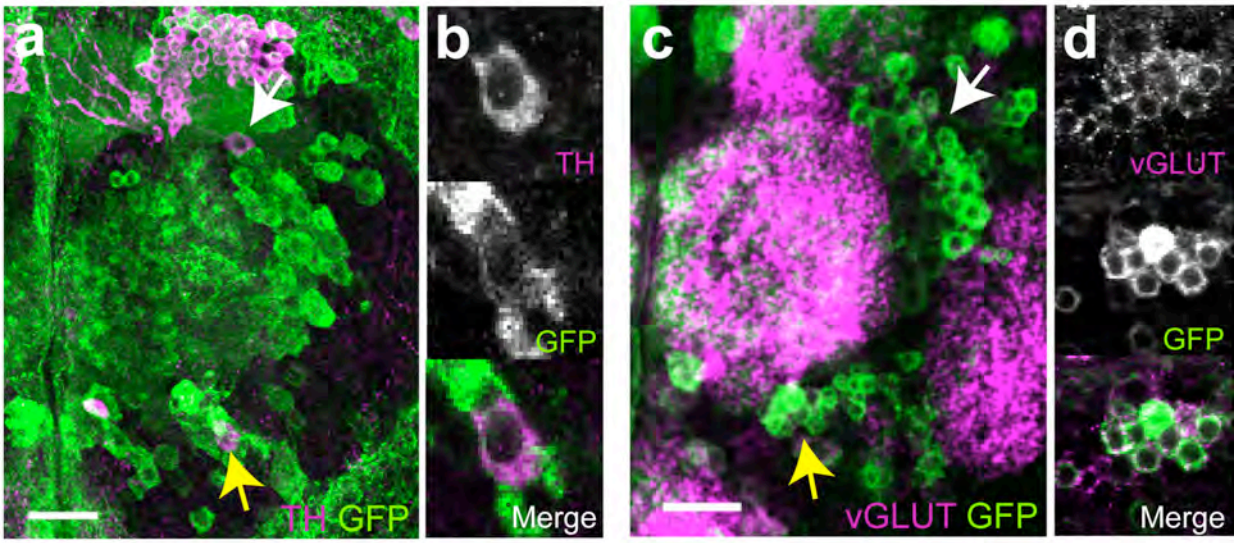


**e**

| | Line3+4+5+10 | | | Line5 | | | Line10 | | |
|---|---|---|---|---|---|---|---|---|---|
| | Lateral cluster | Ventral cluster | Total (n=5) | Lateral cluster | Ventral cluster | Total (n=8) | Lateral cluster | Ventral cluster | Total (n=6) |
| vGLUT+ | 7 ± 3 | 64 ± 7 | 71 ± 7 | 2 ± 2 | 0.3 ± 0.5 | 3 ± 2 | 3 ± 1 | 59 ± 9 | 62 ± 9 |
| vGLUT– | 106 ± 19 | 39 ± 16 | 145 ± 21 | 55 ± 3 | 1 ± 1 | 55 ± 3 | 2 ± 1 | 46 ± 5 | 48 ± 5 |
| Total cells | 113 ± 18 | 103 ± 15 | 216 ± 25 | 57 ± 3 | 1± 2 | 58 ± 3 | 5 ± 1 | 105 ± 8 | 110 ± 8 |

**Supplementary Figure 3. Additional neurotransmitters expressed by LNs.**
(**a-b**) LNs stained with antibody against tyrosine hydroxylase (TH), a marker for dopaminergic neurons. (**a**) A confocal projection with TH-positive cells (magenta) indicated by white and yellow arrows. Green represents mCD8GFP driven by a combination of Lines 3, 4, 5 and 10, which label ~200 LNs described in this study. (**b**) A magnified single confocal section indicated by the yellow arrow in (**a**). We found 2±1 TH-positive cells in the lateral cluster, and 2±1 TH-positive cells in ventral clusters (*n*=12).
(**c-d**) LNs stained with antibody against the vesicular glutamate transporter (vGLUT), a marker for glutamatergic neurons[10]. (**c**) A confocal projection with vGLUT-positive cells (magenta) indicated by white and yellow arrows. Green represents mCD8GFP driven by a combination of Lines 3, 4, 5 and 10. (**d**) A magnified single confocal section indicated by the yellow arrow in (**c**). Scale bars, 20 μm. Genotype, *w; UAS-mCD8GFP/+; H24 GH298/NP3056; OK107/+*.
(**e**) Estimate of the number (mean±SD) of vGLUT-expressing LNs labeled by Lines 3, 4, 5, 10 in combination, or Line 5 and 10 alone.
In separate experiments (data not shown), we found some Line1-labeled neurons in the ventral cluster are vGLUT-positive, but they are not LNs (**Supplementary Fig. 1**). Similarly, no overlap with vGLUT was observed for Lines 3, 4, 6. We did not find any serotonin-immunopositive LNs (data not shown).

Supplementary Figure 4

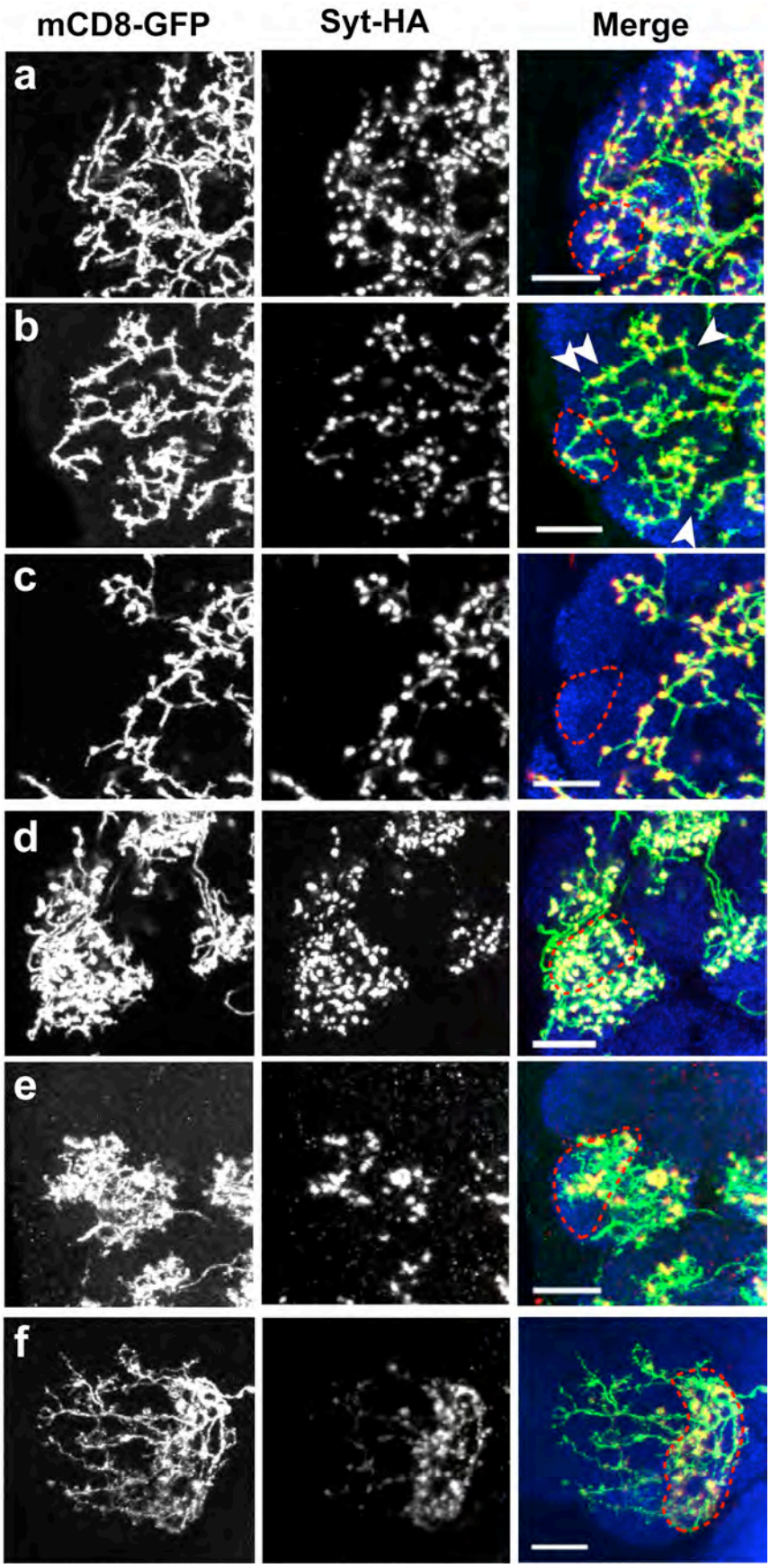

**Supplementary Figure 4. Fine structures of LN processes.**

Despite the overall uniform distribution of synaptotagmin-HA across different glomeruli, the density and subcellular distribution of synaptotagmin-HA puncta differ considerably for different LNs. This figure illustrates some of these differences.

(**a-c**) Three examples of high magnification images from 10 μm projections showing LN processes in medial antennal lobe labeled by mCD8-GFP (left), Syt-HA (middle) and merge (right) with nc82 (blue), mCD8-GFP (green) and Syt-HA (red). The LN processes in (**b**) show spine-like protrusions devoid of Syt-HA (arrowheads), suggesting that they are postsynaptic structures. By contrast, presynaptic Syt-HA puncta are distributed along the process and at the terminals in (**a**) and (**c**). The density of processes varies from sparse (**c**) to intermediate (**b**) to dense (**a**). Dotted lines outline glomerulus VM7.

(**d-e**) Different process densities and Syt-HA distributions in patchy cells. High magnification images from 10 μm projections covering VM7 (dotted line) show dense processes and Syt-HA puncta in (**d**) (mostly labeled by Line1) and less compact processes and a sparse, uneven distribution of Syt-HA puncta in (**e**) (mostly labeled by Line5).

(**f**) High magnification images from 20 μm projections covering glomerulus VP3 (dotted line) from a few-glomerular innervation LN illustrating enrichment of syt-HA puncta in only a subset of processes within the VP3 glomerulus.

Scale bars, 10 μm.

(**a**)-(**f**) correspond to cells in **Fig**. **2a** (left), **2b** (left), **2b** (sixth from left), **2d** (third from left), **2d** (fifth from left) **and 2e** (second from left), respectively.

# Supplementary Figure 5

| a Cell Type | b N | c Gal4s labeling | d Birth window (h AEL) | e No of glomeruli innervated | f Percentage of samples innervating (100 / 76-99 / 51-75 / 26-50 / 1-25 / 0) | g Representative images of cell |
|---|---|---|---|---|---|---|
| Pan glomerular | 290 | Line 1-10 | 0-196 | 54 |  | 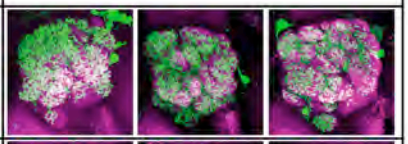 |
| Pheromonal avoiding | 234 | Line 1-9 | 0-76 | 50±3 |  | 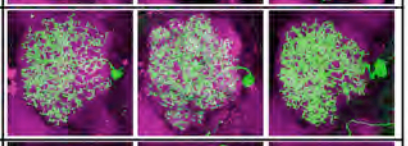 |
| DM avoiding | 41 | Line 2,3,5 | 12-76 | 48±2 |  | 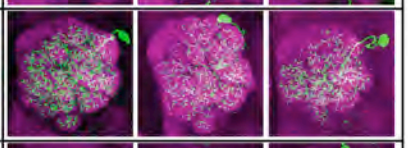 |
| DA avoiding | 47 | Line 1-3,5,7 | 0-120 | 45±3 |  | 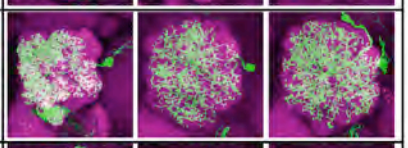 |
| Patchy | 161 | Line 1,3,5 | 22-84 | 30±6 |  |  |
| Dumbbell | 69 | Line 1,2,9 | 18-72 | 33±3 |  | 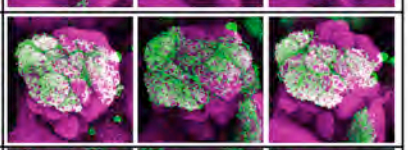 |
| Lateral | 5 | Line 2,3,5 | 50-98 | 31±3 |  | 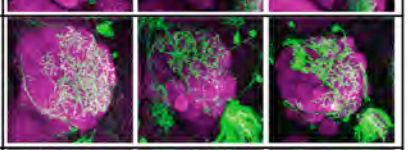 |
| Posterior | 16 | Line 1-3,5,7,10 | 0-196 | 19±5 |  | 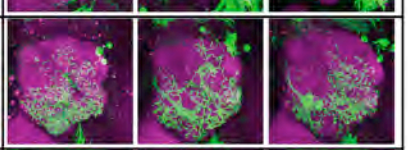 |
| Few glomerular | 58 | Line 1-3,5,10 | 0-192 | 4±2 | 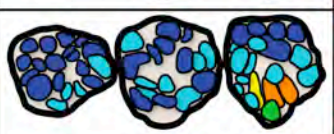 |  |

**h**

| Glomeruli avoided | N | Gal4s labeling | Birth window | No of glomeruli innervated |
|---|---|---|---|---|
| DL3 & DM5 | 30 | Line 1,3-5 | 0-72 | 51±1 |
| DL3 | 90 | Line 1-7, 9 | 0-96 | 51±1 |
| VM6 | 31 | Line 1-6 | 0-76 | 53±1 |
| DM5 | 81 | Line 1,3-6, 9 | 0-120 | 52±1 |
| VL1 | 49 | Line1-6 | 16-180 | 50±2 |
| VP3 | 27 | Line1-3 | 24-72 | 50±3 |
| VM4 | 17 | Line1,3-6,8,9 | 20-120 | 50±3 |

**Supplementary Figure 5. Morphologically distinct LN types and their innervation patterns.**

(**a-g**) Based on clustering (see Methods), we conservatively estimate that there are at least 9 morphologically distinct types of ipsilaterally projecting LNs. (**a-e**) Columns summarizing cell types, the number of cells of that type observed in the dataset, the heat-shock window (in hours after egg laying) during which LNs of a given type are born, the Gal4s labeling a given cell type and the average number (± SD) of glomeruli innervated by a given type of LN. (**f**) Antennal lobe diagrams (see **Fig. 4b** for glomerular names) shaded to reflect % of samples innervating a given glomerulus for a particular cell type. Glomeruli innervated by 100% of cells are labeled in red, 76-99% in orange, 51-75% in yellow, 26-50% in green, 1-25% in cyan and 0% in blue. (**g**) Representative images of 3 individual LNs for each cell type illustrating the similar morphology of all cells in a particular cluster. mCD8GFP in green and nc82/N-cadherin staining in magenta. Scale bar, 20 μM.

(**h**) Table summarizing data as in (**a-e**) for cells that innervate all but a few glomeruli. While it is not clear if all cells that innervate all but a few glomeruli are a single type, there are particular glomeruli that appear to be more likely avoided by these cells, and we observe many samples that do not innervate the listed glomeruli.

It is important to note that the relative frequency of labeling these types of cells does not necessarily reflect the fraction of these cells in a given animal because of our sampling bias with regard to Gal4 lines and heatshock windows—the number of MARCM-labeled single cells is not proportional to the number of LNs in a given Gal4 line, and not all developmental windows are equally sampled.

Supplementary Figure 6

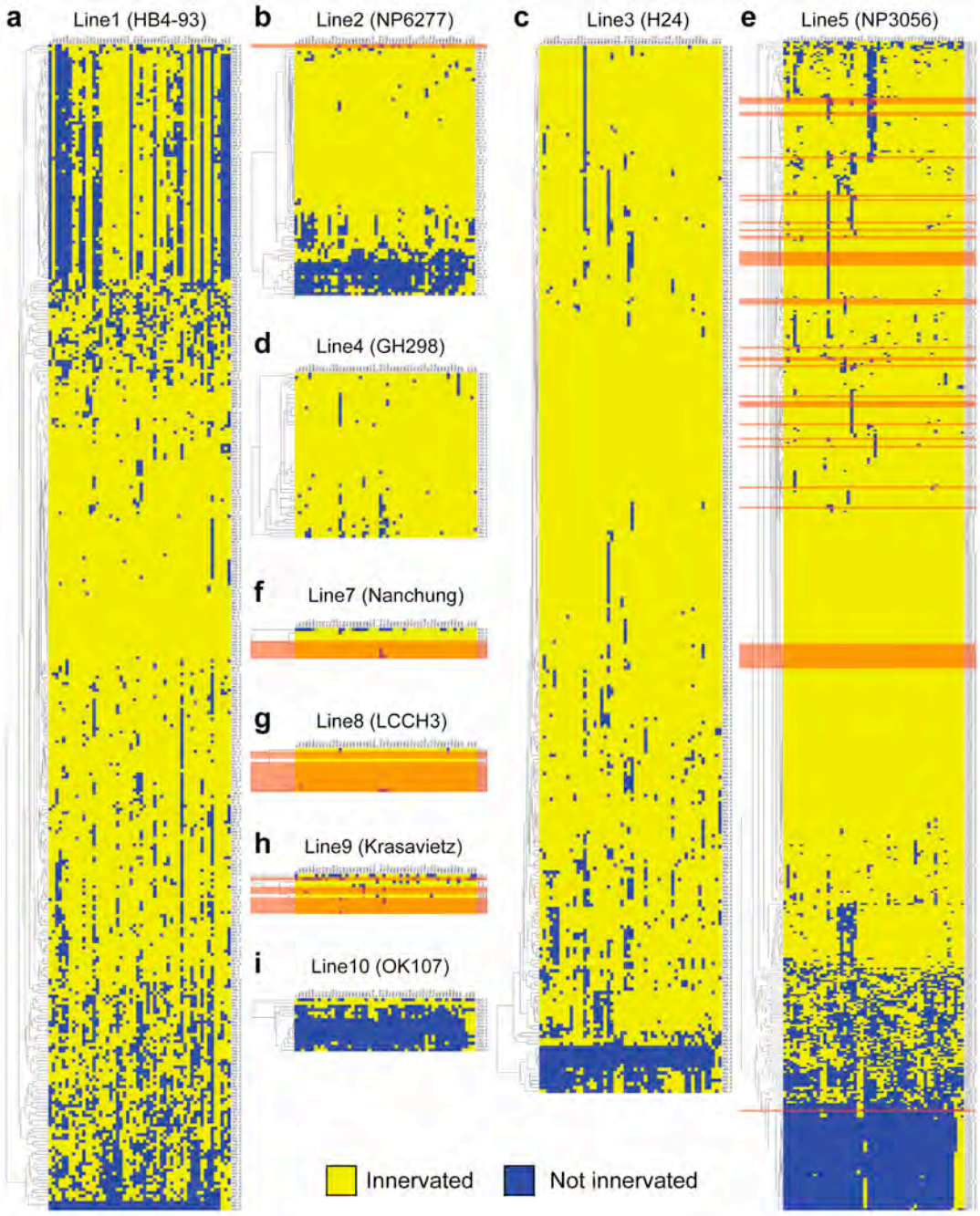


**Supplementary Figure 6. Clustering of LNs by Gal4 lines.**
LNs were divided into subsets based on Gal4 lines. Individual subsets of LNs were then clustered. Line1 (*n*=362) (**a**), Line2 (*n*=75) (**b**), Line3 (*n*=287) (**c**), Line4 (*n*=49) (**d**), Line5 (*n*=578) (**d**), Line6 (*n*=131) (**Fig. 6a**), Line7 (*n*=9) (**f**), Line8 (*n*=13) (**g**) and Line9 (*n*=12) (**h**) label many types of ipsilaterally projecting LNs. Line10 (*n*=16) (**i**) labels a diverse set of mostly bilaterally projecting LNs (see **Supplementary Fig. 9**); only ispilateral innervation patterns are shown here. Innervation patterns of dye filled cells from patch-clamp recordings are highlighted by orange boxes for Lines 2, 5, 7, 8 and 9. Note that the recordings are biased against the patchy LNs and the LNs that innervate only a few glomeruli (see **Methods**).

Supplementary Figure 7

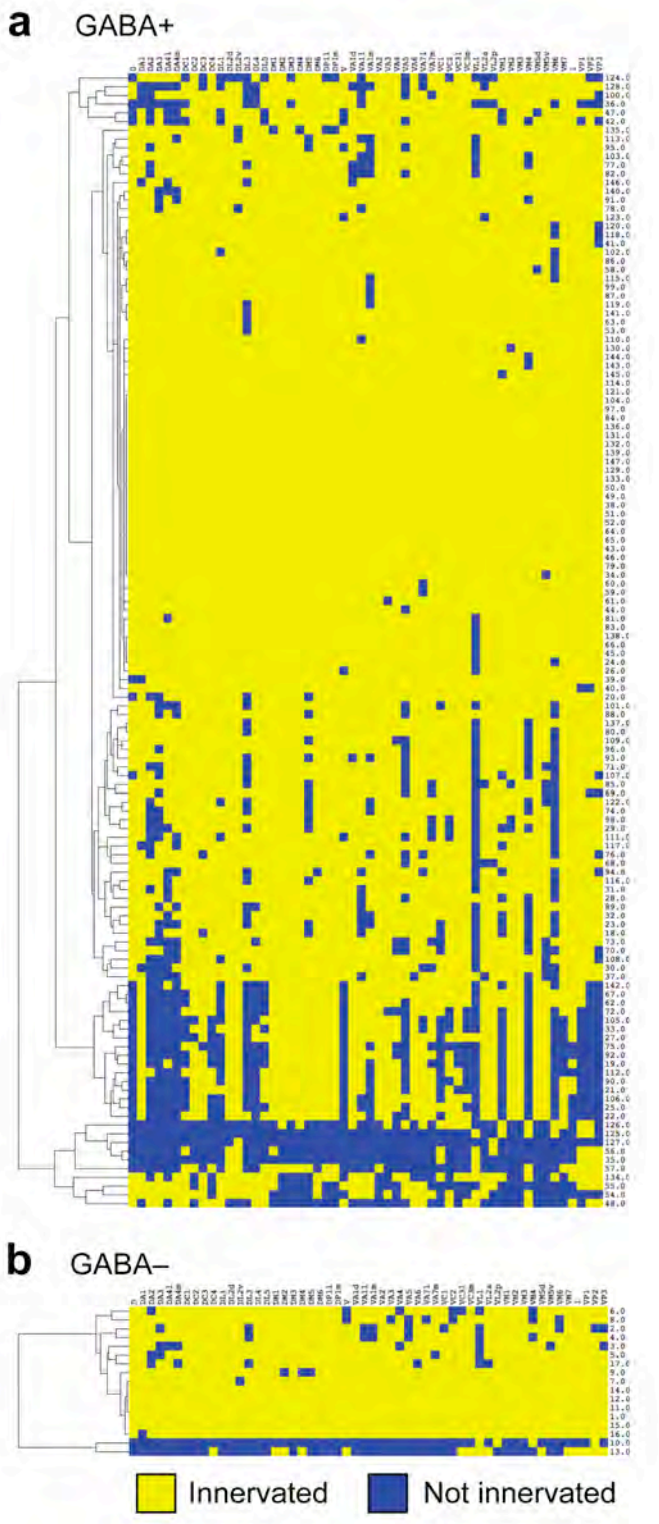


**Supplementary Figure 7. Clustering of GABA+ and GABA– LNs.**
A subset of our MARCM single cell clones were costained with anti-GABA antibody. (**a**) GABA+ (*n*=130) and (**b**) GABA– cells (*n*=17) were clustered separately to gain insight into which types of cells express GABA.

Supplementary Figure 8

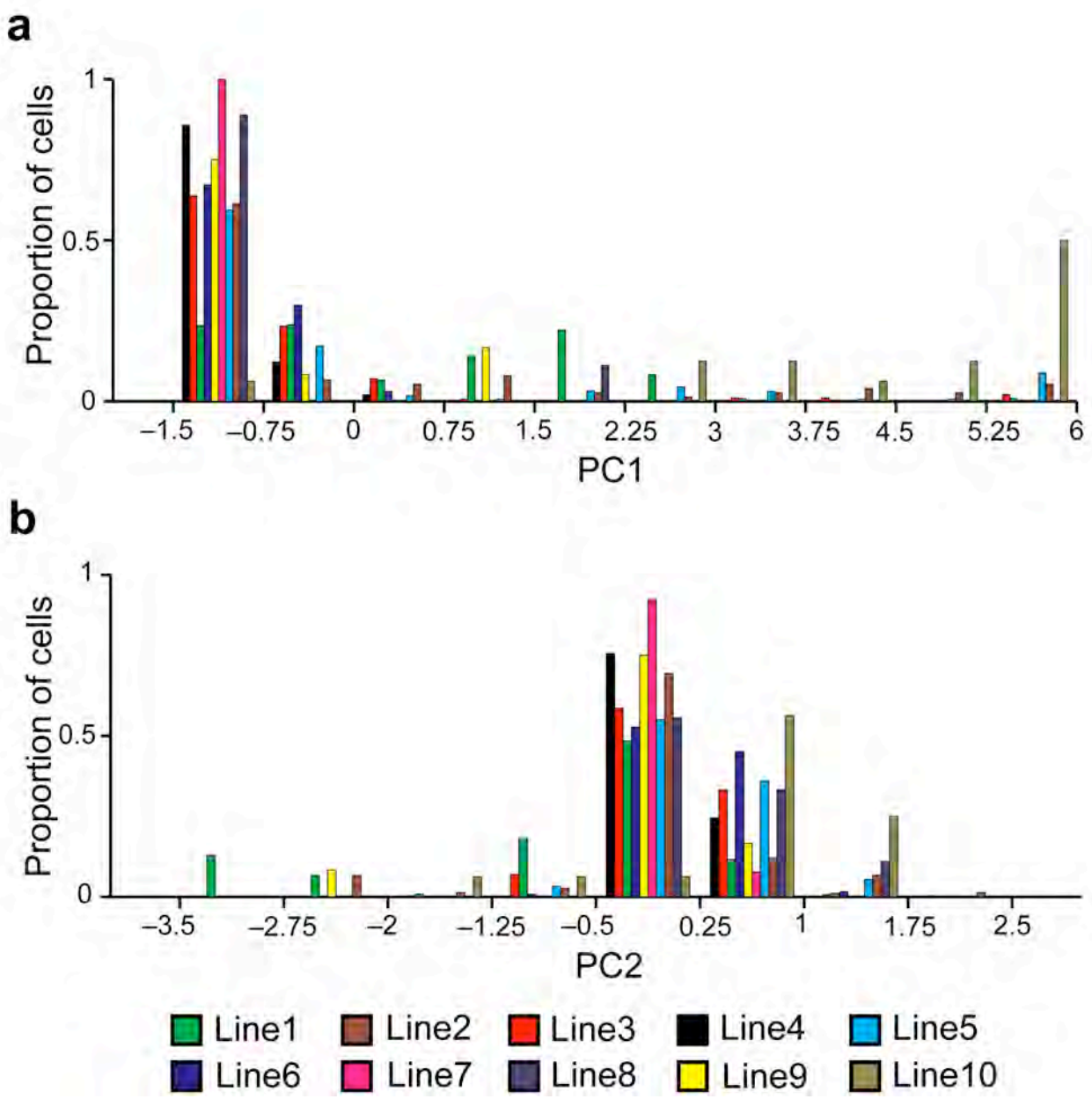


**Supplementary Figure 8. LN distribution over PC1 and PC2 by Gal4 lines.**
(**a**) Histogram of the proportion of cells from each Gal4 distributed over principle component 1 (PC1). Recall that PC1 is anticorrelated with glomerular innervation: cells with large PC1 values innervate few glomeruli. Line10 cells are concentrated at larger values of PC1, reflecting the large number of few-glomerular cells labeled by Line10. LNs labeled by most Gal4 lines are concentrated at low PC1 values.
(**b**) Histogram of the proportion of cells from each Gal4 distributed over PC2. Recall that PC2 is a proxy for membership in the dumbbell class of LNs: cells with large negative values of PC2 are dumbbell cells.
Histograms are binned with a unit of 0.75 and bin edges are indicated on the x-axes. Fractions of LNs labeled by each Gal4 line are plotted separately within each bin. Gal4 lines are color coded at the bottom.

Supplementary Figure 9

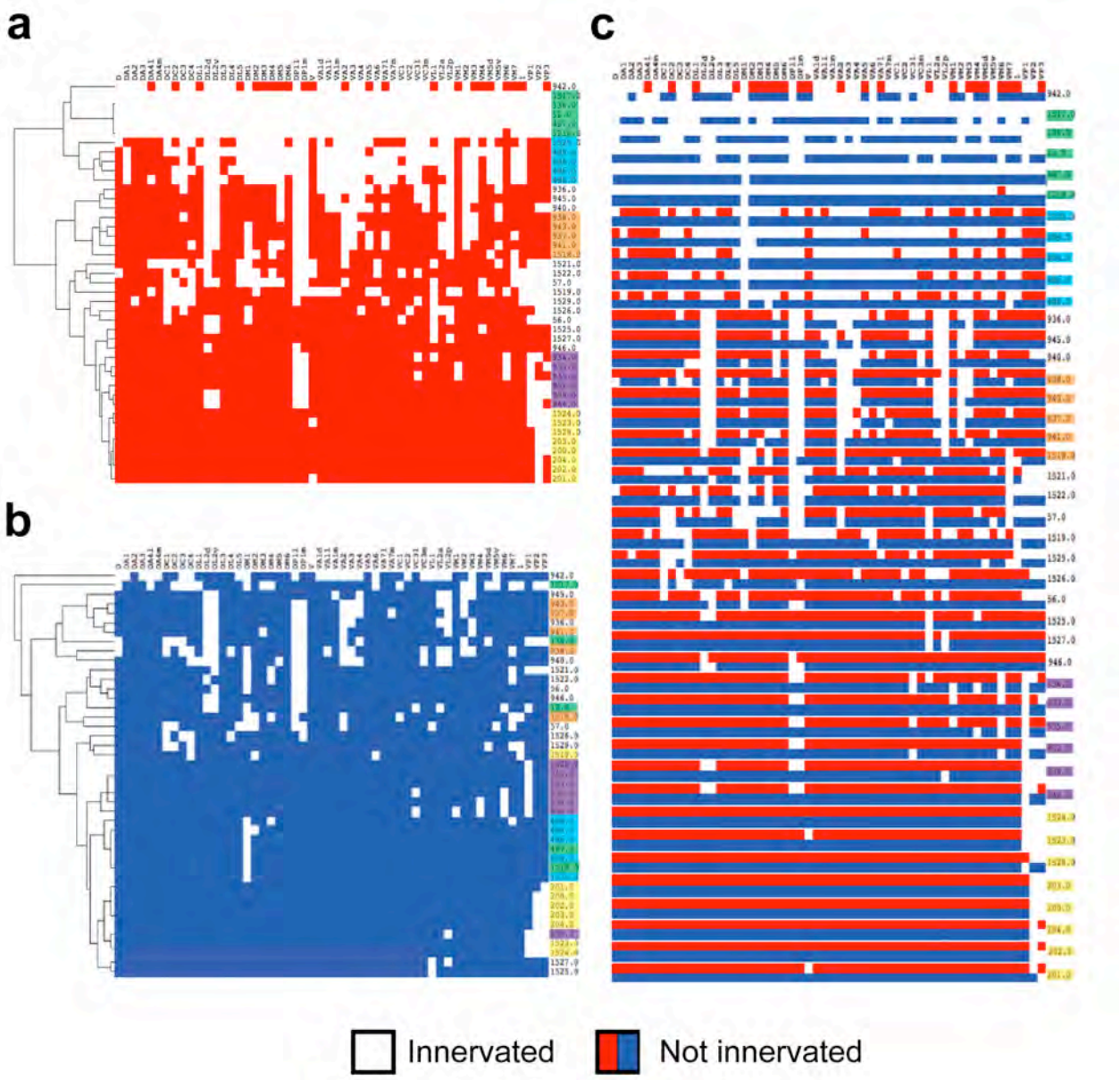


**Supplementary Figure 9. Relationship between ipsilateral and contralateral innervation patterns of bilaterally projecting LNs.**
(**a**) Clustering of bilateral LNs according to ipsilateral glomerular innervation patterns. (**b**) Clustering of bilateral LNs according to contralateral glomerular innervation patterns. Colors on the right mark cells in the same cluster in (**a**), and the corresponding cells in (**b**). (**c**) Alignment of contralateral glomerular innervation patterns with ipsilateral innervation patterns. The contralateral innervation pattern (blue) of each cell is beneath the corresponding ipsilateral innervation pattern (red). Clustering is according to (**a**). With the exception of LNs with pan-glomerular or regional ipsilateral innervation, most bilateral LNs have rather symmetrical glomerular innervation patterns in ipsilateral and contralateral antennal lobes (they differ by 1 or few glomeruli). Ipsi- and contralateral patterns were significantly correlated (Pearson's correlation coefficient, $r$ = 0.46±0.05 (SEM), p<0.01, $n$=38).

Supplementary Figure 10

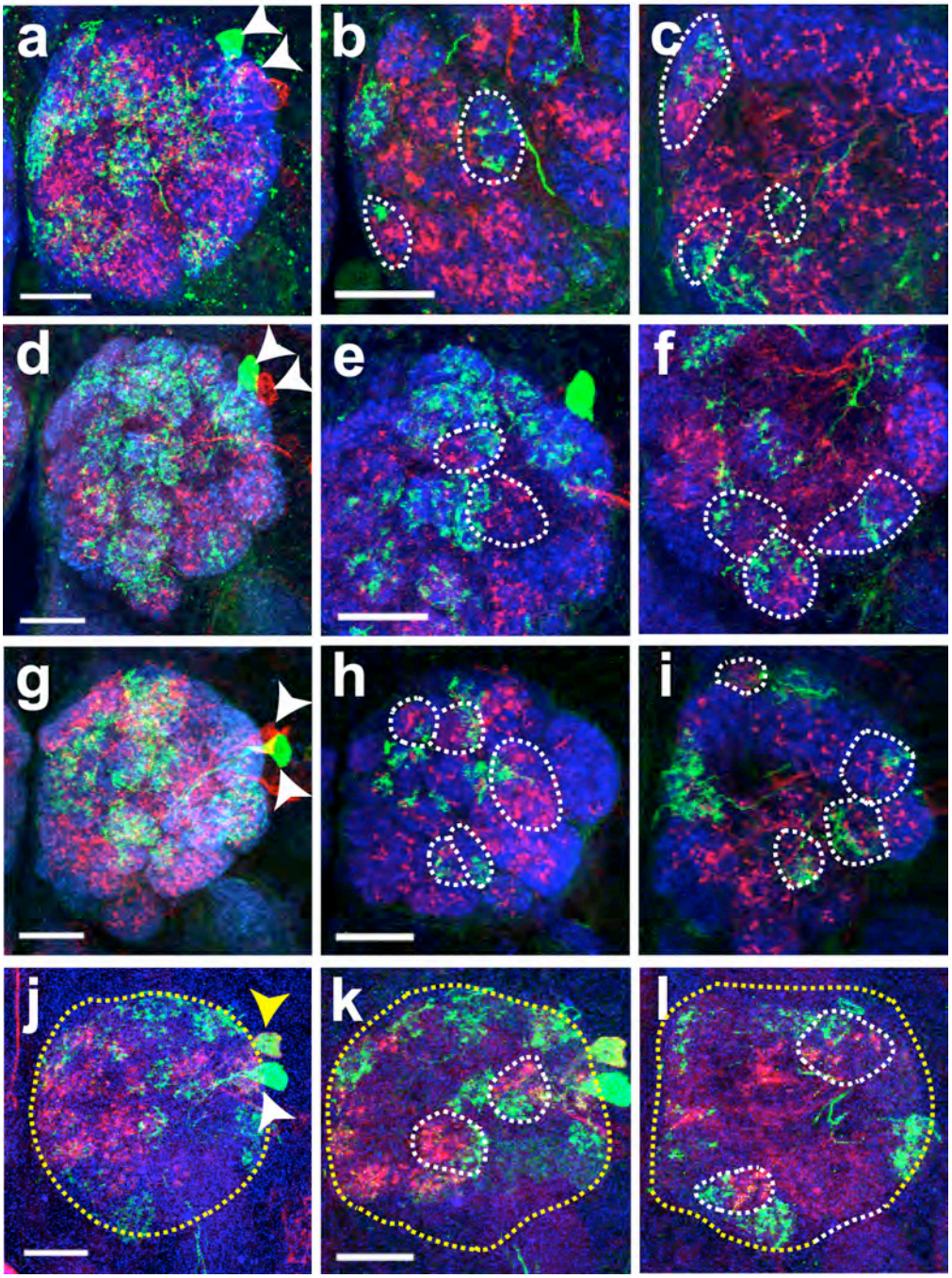


**Supplementary Figure 10. Additional two-cell clones of patchy LNs.**
(**a**, **d**, **g**, **j**) Images showing projections of patchy LN 2-cell clones in the whole antennal lobe with N-cadherin (blue), GFP (green) and CD2 (red) staining.
(**b-c**, **e-f**, **h-i**, **k-l**) 5 μm projections of anterior (**b**, **e**, **h**, **k**) and posterior (**c**, **f**, **i**, **l**) regions of the antennal lobe showing non-overlapped processes of 2 sister patchy cells from (**a**), (**d**), (**g**) and (**j**), respectively. Dashed white lines mark the outline of glomeruli. Dashed yellow lines mark the outline of the antennal lobe. Arrowheads indicate the cell bodies of 2 sister patchy cells. Scale bars, 20 μm.

Supplementary Figure 11

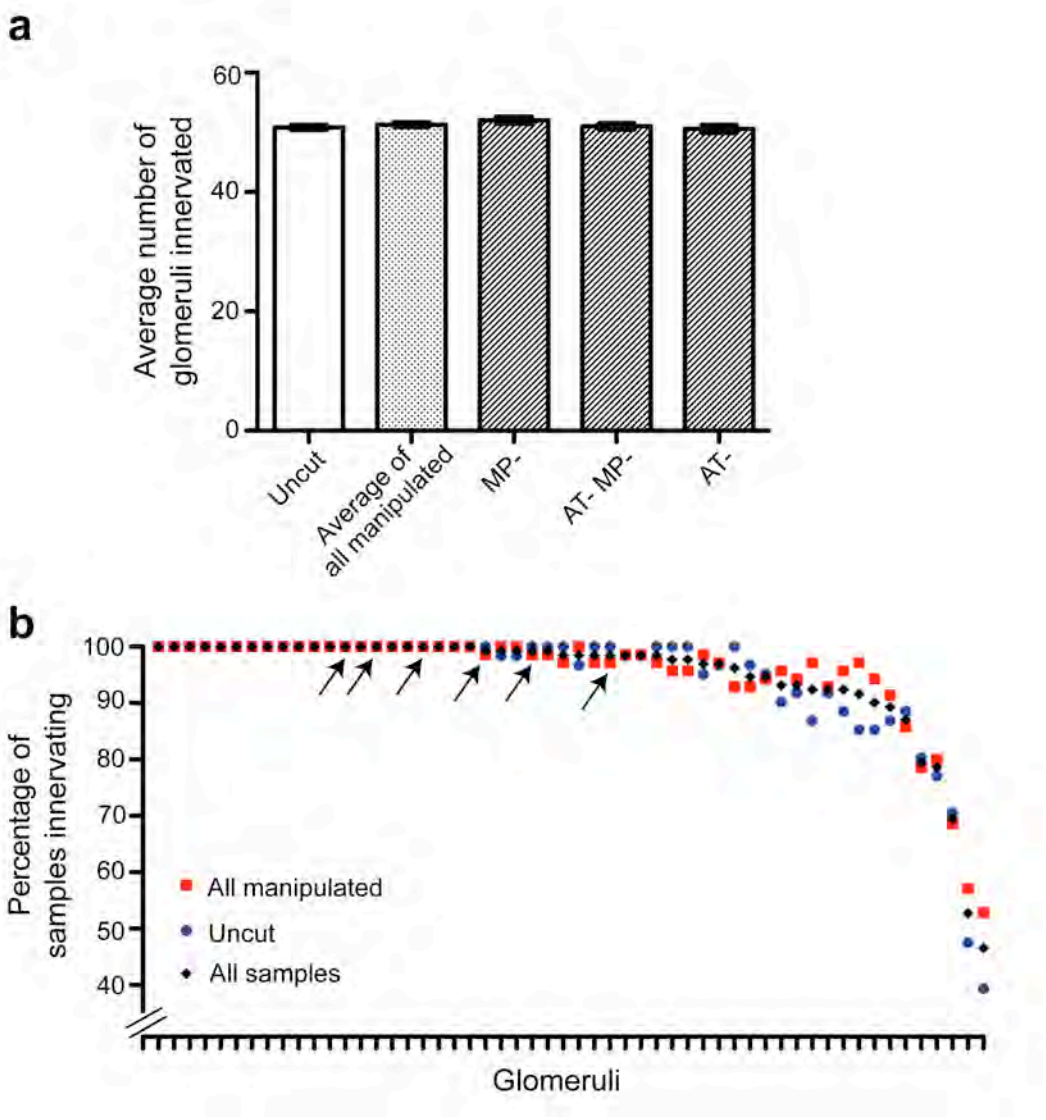


**Supplementary Figure 11. Loss of adult ORN innervation does not affect glomerular innervation variability of Line6 LNs.**
To determine the impact of ORN presence in adults on Line6 innervation variability, we removed the maxillary palps, the antennae or both sets of organs between 0-2 days after eclosion. A complete loss of ORNs by removal of both antennae and maxillary palps does not significantly alter the variability of LN6 innervation patterns.
(**a**) There is no significant difference when comparing the average number of glomeruli innervated by single cell clones for a given experimental condition (ANOVA, p=0.287, F=1.26). uncut, *n*=61; MP-, *n*=24; AT-MP-, *n*=37; AT-, *n*=9.
(**b**) There is no significant difference in the percent of samples that innervate individual glomeruli between uncut (blue) and manipulated samples (red) (ANOVA, p=0.0926, F=2.434). Arrows point to glomeruli innervated by maxillary palp ORNs (from left to right: VA4, VC1, VM7, 1, VC2 and VA7l); maxillary palps have been removed for most manipulated samples (61/70), yet innervation frequency remains similar to uncut samples. Glomeruli are in the same order shown in **Fig. 6f**.

## SUPPLEMANTARY REFERENCES


1. Wilson, R.I. & Laurent, G. Role of GABAergic inhibition in shaping odor-evoked spatiotemporal patterns in the Drosophila antennal lobe. *J Neurosci* **25**, 9069-79 (2005).
2. Shang, Y., Claridge-Chang, A., Sjulson, L., Pypaert, M. & Miesenbock, G. Excitatory local circuits and their implications for olfactory processing in the fly antennal lobe. *Cell* **128**, 601-12 (2007).
3. Dubnau, J. et al. The staufen/pumilio pathway is involved in Drosophila long-term memory. *Curr Biol* **13**, 286-96 (2003).
4. Martin, J.R., Ernst, R. & Heisenberg, M. Mushroom bodies suppress locomotor activity in Drosophila melanogaster. *Learn Mem* **5**, 179-91 (1998).
5. Lee, T., Lee, A. & Luo, L. Development of the Drosophila mushroom bodies: sequential generation of three distinct types of neurons from a neuroblast. *Development* **126**, 4065-76 (1999).
6. Lai, S.L., Awasaki, T., Ito, K. & Lee, T. Clonal analysis of Drosophila antennal lobe neurons: diverse neuronal architectures in the lateral neuroblast lineage. *Development* **135**, 2883-93 (2008).
7. Kitamoto, T., Xie, X., Wu, C.F. & Salvaterra, P.M. Isolation and characterization of mutants for the vesicular acetylcholine transporter gene in Drosophila melanogaster. *J Neurobiol* **42**, 161-71 (2000).
8. Jefferis, G.S. et al. Comprehensive maps of Drosophila higher olfactory centers: spatially segregated fruit and pheromone representation. *Cell* **128**, 1187-203 (2007).
9. Featherstone, D.E. et al. Presynaptic glutamic acid decarboxylase is required for induction of the postsynaptic receptor field at a glutamatergic synapse. *Neuron* **27**, 71-84 (2000).
10. Daniels, R.W. et al. A single vesicular glutamate transporter is sufficient to fill a synaptic vesicle. *Neuron* **49**, 11-6 (2006).